DESIGN OF FULLY DIGITAL CONTROLLED RECONFIGURABLE DUAL-BEAM CONCENTRIC RING ARRAY ANTENNA USING GRAVITATIONAL SEARCH ALGORITHM

A. Chatterjee and G. K. Mahanti

Department of Electronics and Communication Engineering
National Institute of Technology, Durgapur, India

P. R. S. Mahapatra

Department of Computer Science and Engineering
University of Kalyani, Kalyani, India

Abstract—In this paper, we propose an optimization method based on Gravitational Search Algorithm (GSA) for design of reconfigurable dual-beam concentric ring array of isotropic elements with phase only control of five-bit digital phase shifters. The problem is to find a common radial amplitude distribution using four-bit digital attenuator that will generate three different types of broadsided beam pair in vertical plane: a pencil/pencil beam pair, a pencil/flat-top beam pair and a flat-top/flat-top beam pair (sector pattern) with desired value of side lobe level, first null beam width and ripple. The two patterns differ only in radial discrete phase distribution while sharing a common discrete radial amplitude distribution. The optimum sets of four-bit discrete radial amplitude distribution generated by four-bit digital attenuators and five-bit discrete radial phase distribution generated by five-bit digital phase shifters for obtaining dual radiation patterns are computed by Gravitational Search Algorithm.

1. INTRODUCTION

Multiple radiation patterns from a single antenna array are often required in communication and radar related applications. Generally multiple radiation patterns are obtained by switching between the

excitation phase distributions of the elements while sharing common amplitude distributions. The generation of multiple radiation patterns by a single antenna array with prefixed or common amplitude distribution greatly simplifies the hardware implementation of the feed network, since it is technically easier to design a feed network if the element excitations corresponding to different patterns differ only in phase than if they also differ in amplitude. Several methods of generating phase-only multiple pattern antenna arrays have been described [1–6].

Design of phase-differentiated multiple pattern antenna arrays based on simulated annealing algorithm have been described by Diaz et al. [1]. Durr et al. proposed a phase only pattern synthesis method to generate multiple radiations of pre-fixed amplitude distribution with modified Woodward-Lawson technique [2]. Bucci et al. [3] proposed the method of projection to synthesize reconfigurable array antennas with asymmetrical pencil and flat-top beam patterns using common amplitude and varying phase distributions. The design of a phase-differentiated reconfigurable array [4] using particle swarm optimization in angle domain has been described by Gies and Rahmat-Samii. Mahanti et al. [5] synthesized fully digital controlled reconfigurable linear array antennas. Synthesis of continuous phase-only reconfigurable array was described in [6].

In this paper, we proposed to apply optimization algorithm to generate dual radiation patterns from a concentric ring array [7–18] with desired design specifications by switching the optimum 5-bit discrete radial phase of the array elements while sharing a common optimum 4-bit discrete radial amplitude distribution for both the patterns. The optimum value of discrete radial amplitude and discrete radial phase distribution are computed using Gravitational Search Algorithm (GSA) [19] algorithm. The optimized radial amplitude and radial phase distribution obtained by this method can be directly implemented without further quantization.

2. PROBLEM FORMULATION

Phase-differentiated reconfigurable dual pattern antenna array is based on finding a common optimum amplitude distribution shared by both the patterns. While sharing the optimum common amplitude distribution, the two patterns are generated by switching the optimum phase distribution among the array elements. Three different cases comprising a pencil/pencil beam pair, a pencil/flat-top beam pair and a flat-top/flat-top beam pair with different desired specifications have been considered. In case of a pencil/flat-top beam pair and a

pencil/pencil beam pair, one of the pencil beams is generated with zero degree radial phase distribution. Similarly, the array generates a flat-top/flat-top beam pair by switching between the discrete radial phase distributions of the array elements while sharing a common discrete radial amplitude distribution.

Our objective is to find out common discrete radial amplitude and differing discrete radial phase distributions to get dual radiation patterns of a concentric ring array with desired specifications for all the three cases. All the radial amplitudes are varied in the range of $0 \leq I_m \leq 1$ in steps of $1/2^4$ of a 4-bit digital attenuators and the radial phases are varied in the range of $-180° \leq \phi \leq 180°$ in steps of $360°/2^5$ or $11.25°$ of a 5-bit digital phase shifters. The free space far field pattern of the concentric ring array [12, 13] as shown in Figure 1 on the x-y plane can be expressed as:

$$E(\theta, \varphi) = \sum_{m=1}^{M} \sum_{n=1}^{N_m} I_m e^{j[kr_m \sin\theta \cos(\varphi - \varphi_{mn}) + \phi_m]} \tag{1}$$

Normalized absolute power pattern $P(\theta, \varphi)$ in dB can be expressed as follows:

$$P(\theta, \varphi) = 10 \log_{10} \left[\frac{|E(\theta, \varphi)|}{|E(\theta, \varphi)|_{\max}} \right]^2 = 20 \log_{10} \left[\frac{|E(\theta, \varphi)|}{|E(\theta, \varphi)|_{\max}} \right] \tag{2}$$
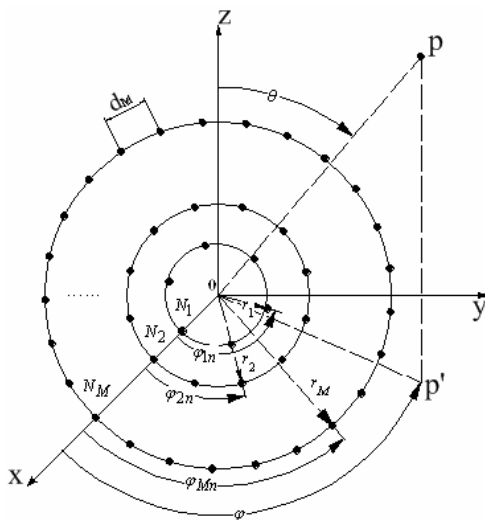

Figure 1. Concentric ring array of isotropic antennas in X-Y plane.

where, M = number of concentric rings, N_m = number of isotropic elements in m-th ring, I_m = excitation amplitude of elements on m-th circular ring, d_m = interelement arc spacing of m-th circle, $r_m = N_m d_m / 2\pi$ is the radius of the mth ring, $\varphi_{mn} = 2n\pi/N_m$ is the angular position of mn-th element with $1 \leq n \leq N_m$, θ, φ = polar, azimuth angle, λ = wave length, k = wave number = $2\pi/\lambda$, j = complex number, ϕ_m = excitation phase of elements on m-th ring.

The fitness functions can be defined as:

$$\text{Fitness1} = \sum_{j=1}^{2} \left(P_{j,o}^{(p1)} - P_{j,d}^{(p1)} \right)^2 H(T1) + \sum_{j=1}^{2} \left(P_{j,o}^{(p2)} - P_{j,d}^{(p2)} \right)^2 H(T2) \quad (3)$$

$$\text{Fitness2} = \sum_{j=1}^{2} \left(P_{j,o}^{(p1)} - P_{j,d}^{(p1)} \right)^2 H(T1) + \sum_{j=1}^{3} \left(P_{j,o}^{(p2)} - P_{j,d}^{(p2)} \right)^2 H(T2) \quad (4)$$

$$\text{Fitness3} = \sum_{j=1}^{3} \left(P_{j,o}^{(p1)} - P_{j,d}^{(p1)} \right)^2 H(T1) + \sum_{j=1}^{3} \left(P_{j,o}^{(p2)} - P_{j,d}^{(p2)} \right)^2 H(T2) \quad (5)$$

where Fitness1 represents the fitness function for the pencil/pencil beam pair, Fitness2 is for the pencil/flat-top beam pair and Fitness3 is for the flat-top/flat-top beam pair. The superscript $p1$ is meant for the design specification of the pattern 1 and the superscript $p2$ is meant for the design specification of the pattern 2 for all the three cases.

$P_{j,o}$ and $P_{j,d}$ represent respectively the obtained and desired values of the parameters for all the three cases given in Table 1, Table 2 and Table 3. The third term of second summation in Equation (4) and also the third term of both the summations in Equation (5) are the ripple parameters for the flat-top beams of second and third cases. The desired tolerance level of the ripple for the flat-top(sector) beam pattern of pencil/flat-top beam pair in the coverage region $-14° \leq \theta \leq 14°$ and for the flat-top beams of the dual flat-top beam pair in the coverage region $-13° \leq \theta \leq 13°$ are kept at 0.5 dB from the peak value of 0 dB.

$H(T1)$ and $H(T2)$ are Heaviside step functions defined as follows:

$$T1 = \left(P_{j,o}^{(p1)} - P_{j,d}^{(p1)} \right) \quad (6)$$

$$T2 = \left(P_{j,o}^{(p2)} - P_{j,d}^{(p2)} \right) \quad (7)$$

$$H(T1) = \begin{cases} 0, & \text{if} \quad T1 < 0, \\ 1, & \text{if} \quad T1 \geq 0 \end{cases} \quad (8)$$

$$H(T2) = \begin{cases} 0, & \text{if} \quad T2 < 0, \\ 1, & \text{if} \quad T2 \geq 0 \end{cases} \quad (9)$$

Table 1. Desired and obtained results for the first case (pencil/pencil beam pair).

Design parameters	Pencil beam 1		Pencil beam 2	
	Desired	Obtained	Desired	Obtained
Side lobe level (dB)	−30.00	−30.7824	−35.00	−35.7694
FNBW (degree)	30.00	28.00	30.00	30.00

Table 2. Desired and obtained results for the second case (pencil/flat-top beam pair).

Design parameters	Pencil beam		Flat-top beam	
	Desired	Obtained	Desired	Obtained
Side lobe level (dB)	−25.00	−26.1881	−25.00	−25.8085
FNBW (degree)	28.00	28.6000	60.00	55.6000
Ripple (dB) $(-14° \leq \theta \leq 14°)$	— — — —	— — — —	0.50	0.7344

Table 3. Desired and obtained results for the third case (flat-top/flat-top beam pair).

Design parameters	Flat-top beam 1		Flat-top beam 2	
	Desired	Obtained	Desired	Obtained
Side lobe level (dB)	−20.00	−21.2295	−25.00	−25.1563
FNBW (degree)	50.00	46.6000	50.00	47.4000
Ripple (dB) $(-13° \leq \theta \leq 13°)$	0.50	0.9220	0.50	0.8917

The weighting factors associated with all the terms in Equation (3), Equation (4) and Equation (5) are made equal to unity. For optimal synthesis of dual-beam concentric ring array the fitness functions of Equation (3), Equation (4) and Equation (5) are to be minimized.

3. GRAVITATIONAL SEARCH ALGORITHM

Gravitational Search Algorithm is a population based search algorithm based on the law of gravity and mass interaction. The algorithm considers agents as objects consisting of different masses. The entire agents move due to the gravitational attraction force acting between them and the progress of the algorithm directs the movements of all agents globally towards the agents with heavier masses. Each agent in GSA is specified by four parameters [19]: position of the mass in d-th dimension, inertia mass, active gravitational mass and passive gravitational mass. The positions of the mass of an agent at specified dimensions represent a solution of the problem and the inertia mass of an agent reflect its resistance to make its movement slow. Both the gravitational mass and the inertial mass, which control the velocity of an agent in specified dimension, are computed by fitness evolution of the problem. The positions of the agents in specified dimensions (solutions) are updated with every iteration and the best fitness along with its corresponding agent is recorded. The termination condition of the algorithm is defined by a fixed amount of iterations, reaching which the algorithm automatically terminates. After termination of the algorithm, the recorded best fitness at final iteration becomes the global fitness for a particular problem and the positions of the mass at specified dimensions of the corresponding agent becomes the global solution of that problem.

Step 1: *Initialization of the agents:*
Initialize the positions of the N number of agents randomly within the given search interval as below:

$$X_i = (x_i^1, \ldots, x_i^d, \ldots, x_i^n), \text{ for } i = 1, 2, \ldots, N. \qquad (10)$$

where, x_i^d represents the positions of the i-th agent in the d-th dimension and n is the space dimension.

Step 2: *Fitness evolution and best fitness computation for each agents:*
Perform the fitness evolution for all agents at each iteration and also compute the best and worst fitness at each iteration defined as below (for minimization problems):

$$\text{best}(t) = \min_{j \in \{1, \ldots, N\}} \text{fit}_j(t) \qquad (11)$$

$$\text{worst}(t) = \max_{j \in \{1, \ldots, N\}} \text{fit}_j(t) \qquad (12)$$

where, $\text{fit}_j(t)$ represents the fitness of the j-th agent at iteration t, $\text{best}(t)$ and $\text{worst}(t)$ represents the best and worst fitness at generation t.

Step 3: *Compute gravitational constant G:*
Compute gravitational constant G at iteration t using the following equation:

$$G(t) = G_0 e^{(-\alpha t/T)} \tag{13}$$

In this problem G_0 is set to 100, α is set to 20 and T is the total number of iterations.

Step 4: *Calculate the mass of the agents:*
Calculate gravitational and inertia masses [19] for each agents at iteration t by the following equations:

$$M_{ai} = M_{pi} = M_{ii} = M_i, \ i = 1, 2, \ldots, N. \tag{14}$$

$$m_i(t) = \frac{\text{fit}_i(t) - \text{worst}_i(t)}{\text{best}(t) - \text{worst}(t)} \tag{15}$$

$$M_i(t) = \frac{m_i(t)}{\sum_{j=1}^{N} m_j(t)} \tag{16}$$

where, M_{ai} is the active gravitational mass of the i-th agent [19], M_{pi} is the passive gravitational mass of the i-th agent [19], M_{ii} is the inertia mass of the i-th agent [19].

Step 5: *Calculate accelerations of the agents:*
Compute the acceleration of the i-th agents at iteration t as below:

$$a_i^d(t) = \frac{F_i^d(t)}{M_{ii}(t)} \tag{17}$$

where, $F_i^d(t)$ is the total force acting on i-th agent calculated as:

$$F_i^d(t) = \sum_{j \in Kbest, \, j \neq i} \text{rand}_j F_{ij}^d(t) \tag{18}$$

Kbest is the set of first K agents with the best fitness value and biggest mass. *Kbest* is computed in such a manner that it decreases linearly with time [19] and at last iteration the value of *Kbest* becomes 2% of the initial number of agents. $F_{ij}^d(t)$ is the force acting on agent 'i' from agent 'j' at d-th dimension and t-th iteration is computed as below:

$$F_{ij}^d(t) = G(t) \frac{M_{pi}(t) \times M_{aj}(t)}{R_{ij}(t) + \varepsilon} \left(x_j^d(t) - x_i^d(t) \right) \tag{19}$$

where, $R_{ij}(t)$ is the Euclidian distance between two agents 'i' and 'j' at iteration t and $G(t)$ is the computed gravitational constant at the same iteration. ε is a small constant.

Step 6: *Update velocity and positions of the agents:*

Compute velocity and the position of the agents at next iteration $(t+1)$ using the following equations:

$$v_i^d(t+1) = \text{rand}_i \times v_i^d(t) + a_i^d(t) \tag{20}$$

$$x_i^d(t+1) = x_i^d(t) + v_i^d(t+1) \tag{21}$$

Step 7: Repeat from steps 2–6 until iterations reaches their maximum limit. Return the best fitness computed at final iteration as a global fitness of the problem and the positions of the corresponding agent at specified dimensions as the global solution of that problem.

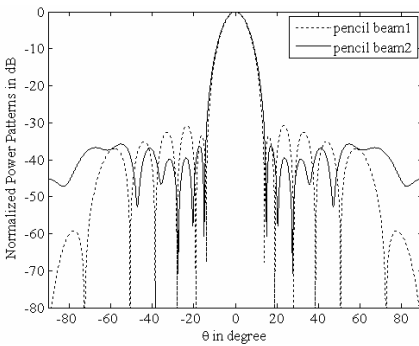In this problem the algorithm is run for 400 iterations and number of agents is taken 50.

Figure 2. Normalized power patterns in dB of the concentric ring array for the pencil/pencil beam pair.
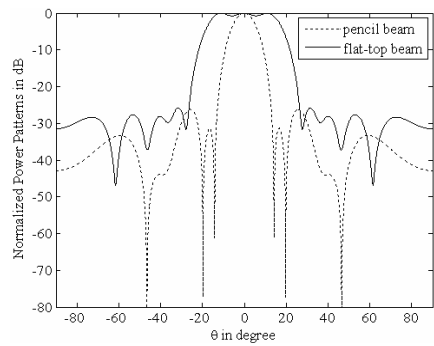

Figure 3. Normalized power patterns in dB of the concentric ring array for the pencil/flat-top beam pair.
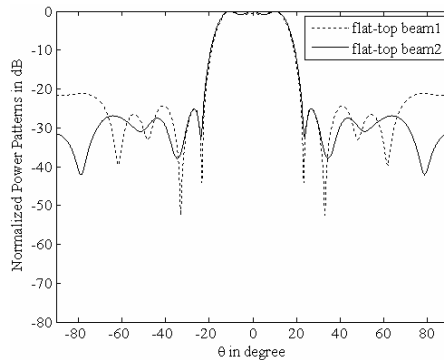

Figure 4. Normalized power patterns in dB of the concentric ring array for the flat-top/flat-top beam pair (sector pattern pair).

4. SIMULATION RESULTS

We consider a ten ring concentric array where the number of element in each ring is taken as multiple of 4, i.e., $4m$, where m is the ring number. The inter-element spacing d_m in each ring are taken as 0.5λ. The radius of the m-th ring of the array when the number of elements in m-th ring N_m and the inter-element distance d_m is known, are determined from the expression $r_m = N_m d_m / 2\pi$. All patterns are optimized in

Table 4. Optimum common discrete radial amplitude and optimum discrete radial phase distributions computed by GSA for the pencil/pencil beam pair.

Ring Number	Pencil beam 1	
	Common Amplitude (4-bit)	Phase (5-bit) (degree)
1	1.0000	0
2	0.9375	0
3	0.8125	0
4	0.7500	0
5	0.5625	0
6	0.6875	0
7	0.1875	0
8	0.5625	0
9	0.1250	0
10	0.3750	0
Ring Number	Pencil beam 2	
	Common Amplitude (4-bit)	Phase (5-bit) (degree)
1	1.0000	-168.7500
2	0.9375	-180.0000
3	0.8125	-157.5000
4	0.7500	180.0000
5	0.5625	-168.7500
6	0.6875	-168.7500
7	0.1875	-168.7500
8	0.5625	-180.0000
9	0.1250	-56.2500
10	0.3750	180.0000

$\varphi = 0°$ plane. The design specifications of the reconfigurable array for the first, second and third cases are shown in Table 1, Table 2 and Table 3 respectively. From Table 1, it can be observed that the obtained values of the design specifications for the pencil /pencil beam pair totally fulfill the desired design specifications. The normalized power patterns of the pencil/pencil beam pair are shown in Figure 2. From Table 2, it can be noticed that the value of the ripple (absolute value) we obtained for the flat-top beam in the region $-14° \leq \theta \leq 14°$

Table 5. Optimum common discrete radial amplitude and optimum discrete radial phase distributions computed by GSA for the pencil/flat-top beam pair.

Ring Number	Pencil beam	
	Common Amplitude (4-bit)	Phase (5-bit) (degree)
1	1.0000	0
2	0.8750	0
3	0.6875	0
4	0.4375	0
5	0.4375	0
6	0.6250	0
7	0.2500	0
8	0.4375	0
9	0.1250	0
10	0.1875	0
Ring Number	Flat-top beam	
	Common Amplitude (4-bit)	Phase (5-bit) (degree)
1	1.0000	-146.2500
2	0.8750	-123.7500
3	0.6875	-146.2500
4	0.4375	-56.2500
5	0.4375	-123.7500
6	0.6250	11.2500
7	0.2500	-101.2500
8	0.4375	33.7500
9	0.1250	-78.7500
10	0.1875	78.7500

is 0.7344 dB, which is 0.2344 dB higher than the desired tolerance of 0.5 dB. All the other obtained design parameters for the pencil/flat-top beam pair fulfill the desired design specifications. The normalized power patterns for the pencil/flat-top beam pair are shown in Figure 3. Table 3 shows that the obtained values of the ripple for the flat-top/flat-top beam pair in the region $-13° \leq \theta \leq 13°$ are 0.9220 dB and 0.8917 dB, which are 0.4220 dB and 0.3917 dB higher than the desire values. The other obtained design parameters totally fulfill the

Table 6. Optimum common discrete radial amplitude and optimum discrete radial phase distributions computed by GSA for the flat-top/flat-top beam pair.

Ring Number	Flat-top beam 1	
	Common Amplitude (4-bit)	Phase (5-bit) (degree)
1	0.9375	146.2500
2	0.9375	146.2500
3	0.5625	112.5000
4	0.6250	157.5000
5	0.3125	45.0000
6	0.2500	135.0000
7	0.3750	-11.2500
8	0.1875	56.2500
9	0.1250	-22.5000
10	0.1875	-22.5000
Ring Number	Flat-top beam 2	
	Common Amplitude (4-bit)	Phase (5-bit) (degree)
1	0.9375	67.5000
2	0.9375	56.2500
3	0.5625	56.2500
4	0.6250	56.2500
5	0.3125	-56.2500
6	0.2500	56.2500
7	0.3750	-67.5000
8	0.1875	-112.5000
9	0.1250	-45.0000
10	0.1875	-101.2500

desired design specifications. The normalized power patterns for the flat-top/flat-top beam pair are shown in Figure 4.

The common discrete radial amplitude and the discrete radial phase distributions of the array computed by GSA for generating radiation patterns: pencil/pencil beam pair, pencil/flat-top beam pair and flat-top/flat-top beam pair with desired design specifications are shown in Table 4, Table 5, and Table 6 respectively.

5. CONCLUSIONS

An optimization technique based on Gravitational Search Algorithm (GSA) for the design of a fully digital controlled reconfigurable concentric ring array antenna has been proposed in this paper. The paper deals with radial variation of amplitude and phase distribution of the elements instead of variation of amplitude and phase of all the elements. This leads to simple feed network design and less computational complexity.

The method presented here takes the values of digital attenuator and digital phase shifter directly into account during synthesis. This leads to better synthesis results, compared to conventional methods where amplitudes and phases are subsequently quantized.

Results clearly show a very good agreement between the desired and GSA synthesized pattern even with a 4-bit digital attenuator and a 5-bit digital phase shifter instead of a continuous phase shifter and an analog attenuator.

Moreover, for practical applications, the design of reconfigurable antenna arrays with all digital control is preferred in order to keep costs low, and maintain accuracy. It is also easier to control the output of digital attenuator and digital phase shifter than its analog counterpart.

It can be easily embedded on printed circuit board and integration with microwave monolithic integrated circuit (MMIC) is also easier. This design method can be used directly in practice to synthesize reconfigurable concentric ring isotropic antenna arrays with all digital control. Results for a concentric ring isotropic antenna array have illustrated the performance of this proposed technique. It can also be used for synthesizing other array configurations.

REFERENCES

1. Diaz, X., J. A. Rodriguez, F. Ares, and E. Moreno, "Design of phase-differentiated multiple-pattern antenna arrays," *Microwave Opt. Technol. Lett.*, Vol. 26, 52–53, Jul. 2000.

2. Durr, M., A. Trastoy, and F. Ares, "Multiple-pattern linear antenna arrays with single prefixed amplitude distributions: Modified Woodward-Lawson synthesis," *Electronics Letters*, Vol. 36, No. 16, 1345–1346, Aug. 2000.

3. Bucci, O. M., G. Mazzarella, and G. Panariello, "Reconfigurable arrays by phase-only control," *IEEE Trans. Antennas and Propag.*, Vol. 39, No. 7, 919–925, Jul. 1991.

4. Gies, D. and Y. Rahmat-samii, "Particle swarm optimization for reconfigurable phase-differentiated array design," *Microwave Opt. Technol. Lett.*, Vol. 38, 168–175, Aug. 2003.

5. Mahanti, G. K., A. Chakraborty, and S. Das, "Design of fully digital controlled reconfigurable array antennas with fixed dynamic range ratio," *Journal of Electromagnetic Waves and Applications*, Vol. 21, No. 1, 97–106, 2007.

6. Mahanti, G. K., A. Chakraborty, and S. Das, "Design of phase-differentiated reconfigurable array antennas with minimum dynamic range ratio," *IEEE Antennas and Wireless Propagation Letters*, Vol. 5, 262–264, Dec. 2006.

7. Stearns, C. and A. Stewart, "An investigation of concentric ring antennas with low sidelobes," *IEEE Trans. Antennas Propag.*, Vol. 13, No. 6, 856–863, Nov. 1965.

8. Goto, N. and D. K. Cheng, "On the synthesis of concentric-ring arrays," *IEEE Proc.*, Vol. 58, No. 5, 839–840, May 1970.

9. Biller, L. and G. Friedman, "Optimization of radiation patterns for an array of concentric ring sources," *IEEE Trans. Audio Electroacoust.*, Vol. 21, No. 1, 57–61, Feb. 1973.

10. Huebner, D., "Design and optimization of small concentric ring arrays," *Proc. IEEE Antennas Propagation Int. Symp.*, Vol. 16, 455–458, May 1978.

11. Kumar, B. P. and G. R. Branner, "Design of low side lobe circular ring array by element radius optimazation," *Proc. IEEE Antennas Propagation Int. Symp.*, 2032–2035, Orlando, FL, Aug. 1999.

12. Dessouky, M. I., H. A. Sharshar, and Y. A. Albagory, "Efficient sidelobe reduction technique for small-sized concentric circular arrays," *Progress In Electromagnetics Research*, Vol. 65, 187–200, 2006.

13. Haupt, R. L., "Optimized element spacing for low side lobe concentric ring arrays," *IEEE Trans. Antennas Propag.*, Vol. 56, No. 1, 266–268, Jan. 2008.

14. Pathak, N., G. K. Mahanti, S. K. Singh, J. K. Mishra, and A. Chakraborty, "Synthesis of thinned planar circular array

antennas using modified particle swarm optimization," *Progress In Electromagnetics Research Letters*, Vol. 12, 87–97, 2009.

15. Chatterjee, A., G. K. Mahanti, and N. Pathak, "Comparative performance of gravitational search algorithm and modified particle swarm optimization algorithm for synthesis of thinned scanned concentric ring array antenna," *Progress In Electromagnetics Research B*, Vol. 25, 331–348, 2010.

16. Dessouky, M. I., H. A. Sharshar, and Y. A. Albagory, "Optimum normalized-Gaussian tapering window for side lobe reduction in uniform concentric circular arrays," *Progress In Electromagnetics Research*, Vol. 69, 35–46, 2007.

17. Dessouky, M., H. Sharshar, and Y. Albagory, "A novel tapered beamforming window for uniform concentric circular arrays," *Journal of Electromagnetic Waves and Applications*, Vol. 20, No. 14, 2077–2089, 2006.

18. Chen, T. B., Y. L. Dong, Y. C. Jiao, and F. S. Zhang, "Synthesis of circular antenna array using crossed particle swarm optimization algorithm," *Journal of Electromagnetic Waves and Applications*, Vol. 20, No. 13, 1785–1795, 2006.

19. Rashedi, E., H. Nezamabadi-Pour, and S. Saryazdi, *GSA: A Gravitational Search Algorithm*, Vol. 179, No. 13, 2232–2248, Information Sciences, 2009.